

Volume 09 Issue 02 2025

Research Article https://doi.org/10.56979/902/2025

Enhancement of 3D Object Detection Using Deep Learning

Muhammad Hamza¹, Muhammad Javed Iqbal¹, Muhammad Munawar Iqbal¹, Shahbaz Pervez Chattha², and Seyed Ebrahim Hosseini²

¹Department of Computer Science, University of Engineering and Technology Taxila, 47080, Pakistan.

²School of Applied IT, Whitecliffe Christchurch, New Zealand.

*Corresponding Author: Muhammad Munawar Iqbal. Email: munwariq@gmail.com

Received: June 15, 2025 Accepted: August 26, 2025

Abstract: 3D printing, an advanced form of additive manufacturing, has revolutionized production by enabling the creation of complex, customized objects used across industries like aerospace, healthcare, and automotive. Despite its benefits, 3D printing faces challenges such as defects (cracks, warping, surface imperfections) that compromise the structural integrity of printed objects, especially in high-precision applications. Traditional defect detection methods rely on manual inspection or image processing, which are time-consuming and error-prone. To address these issues, deep learning has been applied for automated defect detection. The proposed model, DenseNet201, is a pre-trained convolutional neural network (CNN), fine-tuned on a 3D printing defect dataset to classify defects and non-defects. Enhanced techniques, such as data augmentation, dropout regularization, and optimizer tuning (using the Adam optimizer), are implemented to optimize the model's performance. These methods contribute to the enhancement of 3D printing quality by improving defect detection accuracy. The trained model achieved maximum accuracy 93%, it also shows balanced performance across all classes with a score of 0.92 for average precision, recall, and F1 score; while showing the best performance on key defect types with F1 scores of 0.98 and 0.93 displaying strong defect detection which ultimately enhances manufacturing efficiency, reduces waste, and minimizes costs associated with traditional inspection methods. This approach aligns with the goal of utilizing deep learning to significantly improve the quality control process in 3D object detection.

Keywords: Three-Dimensional (3D) Printing; Deep Learning (DL); Convolutional Neural Networks (CNN); Transfer Learning

1. Introduction

3D printing [1], or additive manufacturing, has become a transformative manufacturing approach by enabling the precise fabrication of complex, customized components across industries such as aerospace, healthcare, and automotive. Despite its versatility, a persistent challenge remains in ensuring product reliability due to surface and structural defects [2] such as cracks, warping, and layer shifting that frequently emerge during fabrication. These defects directly affect dimensional accuracy and mechanical strength, making automated and scalable defect detection [3] essential for maintaining industrial production quality. However, current quality inspection methods still rely heavily on manual observation or simple image processing, which limits scalability and accuracy in large-scale or high-precision environments.

The conventional defect-detection approaches, such as manual scrutiny and image processing, are sometimes tedious, labor-demanding, and prone to error because of the involvement of humans. These techniques have limited scalability and cannot be used to deal with large-scale quantities of prints or very sophisticated objects. With the development of 3d printing technology, there is an increased importance

that a solution to the detection of defects be automated and is both accurate and scalable. The issue can be solved with the help of deep learning [4]. Deep learning models have the ability to identify and classify defects in 3D printing artifacts with a high rate of accuracy using advanced convolutional neural networks (CNNs) [5].

The proposed methodology applies deep learning to enhance quality control in 3D printing by fine-tuning the DenseNet201 model [6] on a 3D printing defect dataset. DenseNet201 was specifically selected for its dense connectivity pattern, which enables efficient feature reuse and gradient flow, minimizing vanishing gradients while improving learning efficiency compared to conventional CNNs. Its deep-layered architecture allows the extraction of fine-grained texture and geometric details critical for distinguishing subtle surface defects in printed objects. Through data augmentation, dropout regularization, and adaptive optimization using the Adam optimizer, the model achieves high classification accuracy and stable convergence, ensuring reliable post-fabrication defect detection.

This paper presents a deep learning-based 3D object defect detection framework designed to reduce manual inspection while improving accuracy and efficiency in industrial quality control. Using state-of-the-art neural architectures and a transfer learning strategy, the proposed framework addresses common challenges in 3D object defect detection, including variable lighting, geometric distortions, and occlusion effects. The developed training and evaluation pipeline is calibrated for practical post-fabrication inspection of 3D printed components and aligns with industrial standards for quality assurance. Although this study focuses on post-print defect detection, it establishes a foundation for future integration with real-time monitoring systems to enable in-process quality control.

The rest of the article is organized as follows: The Literature review is described in section 2. Section 3 presents the proposed methodology. Result & issue discussion is made in Section 4. Finally, the Conclusion & Future work is discussed in Section 5.

2. Literature Review

The literature review examines the integration of artificial intelligence (AI) and deep learning (DL) techniques [7] within 3D printing quality control systems [8], emphasizing their evolving role in automated defect detection [9]. While AI [10] and DL [11] have advanced productivity and automation across manufacturing, their application to 3D printing defect analysis remains constrained by limited datasets, inconsistent evaluation standards, and low scalability of inspection methods. Conventional image-processing or handcrafted-feature approaches often fail to generalize across diverse printer settings and materials.

Convolutional neural networks (CNNs) [12] have demonstrated superior capability in extracting spatial and texture-based information from image data [13], enabling object and surface defect detection in industrial contexts [14]. However, most existing CNN-based studies [15] on 3D printing, focus on single defect types or rely on custom datasets, making cross-platform deployment difficult. Likewise, transfer learning offers a practical solution by adapting pre-trained models to small, domain-specific datasets, yet prior works rarely explore how fine-tuned architectures can achieve balanced accuracy across multiple defect classes [16]. This gap motivates the present study, which applies a fine-tuned DenseNet201 model [17] to address scalability, multi-class imbalance, and robustness issues in 3D-printed object inspection. Here we explore the fundamental technologies behind 3D printing. It includes a detailed explanation of various 3D printing technologies[18], their applications, and their benefits in different industries. One of the most popular and reasonably priced 3D printing methods for production and prototyping is Fused Deposition Method (FDM) [19]. FDM is ideal for applications where low-cost, quick prototyping, and functional parts are required. Stereolithography (SLA) [20] cures liquid resin into solid layers using ultraviolet (UV) light. It is appropriate for applications needing complex designs, such as those in the jewelry and dental sectors, because it provides more precision and fine detailing than FDM. Selective Laser Sintering (SLS) technology [21] uses a laser to fuse powdered material into solid layers. SLS is typically used for industrial-grade products that require durable and high-performance materials.

Li, V. et al [22] proposed an augmented reality (AR)-integrated 3D object detection framework to enhance scene awareness in autonomous driving environments. The approach combines real-world perception with AR-assisted virtual augmentation to improve spatial understanding and detection accuracy. Using the KITTI and nuScenes datasets, the method achieved an accuracy of 92%, outperforming conventional

LiDAR camera fusion systems. The inclusion of AR layers enables more comprehensive contextual awareness, particularly in complex traffic scenes. However, the system's reliance on specialized AR hardware makes its large-scale deployment challenging and hardware-dependent.

Li, Z. et al. [23] The framework, presented at CVPR 2025, focuses on improving occlusion handling in 3D vision tasks through geometry-optimized neural radiance fields (NeRF). By leveraging multi-view images, the model reconstructs fine-grained scene geometry and enhances 3D object localization accuracy. Experimental results demonstrated an accuracy of 91%, showing significant improvement in voxel-level reconstruction compared to baseline detectors. Despite its strong geometric consistency and robustness under occlusion, the approach incurs high computational costs, limiting its real-time applicability in embedded or mobile systems.

The Memory-Augmented Detection (MAD) framework, Agro, B. et al [24] introduces a temporal memory mechanism to address occlusion and continuity issues in sequential LiDAR data. The model integrates historical features using a memory bank to maintain contextual information over time, leading to improved detection performance in partially visible or occluded scenes. Evaluations on LiDAR sequence datasets demonstrated an 88% accuracy, highlighting substantial gains in recall under dynamic conditions. However, the model's increased latency and higher computational demand due to temporal alignment represent major challenges for real-time applications.

Xia, B. et al. [25] developed a multi-modal fusion approach to enhance object detection performance in complex driving environments. The framework combines image, LiDAR, and roadside sensor data to create a unified representation that captures both spatial and semantic features. Experiments on the KITTI and custom multi-sensor datasets reported an 88% accuracy, demonstrating superior robustness under varying lighting and weather conditions. While the fusion strategy improves detection precision and recall, it requires multiple synchronized sensors, making the system costly and technically demanding to implement in practical settings.

Song, S.-H. et al. [26] proposed a diverse knowledge distillation strategy to improve sparse-input 3D object detection. The approach employs multiple teacher networks with complementary representations to guide a student detector trained on 4D Radar Tensor (4DRT) data. The technique achieved an accuracy of 77.3%, marking a 7.3% AP₃D improvement over the baseline. This method effectively compensates for sparse input modalities by distilling diverse spatial knowledge. However, the framework introduces high training complexity, as it requires managing multiple teacher models and large-scale data interactions during training.

Li, S. et al. [27] introduced the Adversarial Adaptive Data Augmentation (AADA) strategy to improve 3D object detection robustness against lighting changes and occlusions. The method generates adversarial perturbations that enhance model adaptability across varying environmental conditions. Trained and tested on the KITTI and nuScenes datasets, the approach achieved an accuracy of 73.8%, reflecting a 0.8% mAP improvement over traditional augmentation techniques. Despite its improved generalization ability, the AADA framework demands careful hyperparameter tuning and introduces additional computational overhead during training. Table 1 presents a critical summary of the literature review.

Table 1. Summary of relevant literature review

		diffilliary of it	cicvant incrature		
Reference	Problem	Dataset	Technique	Performance	Limitation
	Statement			Evaluation	
[22]	Enhance scene	KITTI,	AR-integrated	92 %	Hardware
	awareness in	nuScenes	3D detection		dependent
	autonomous driving	5			
[23]	Enhance occlusion	Multi-view	NeRF-based	91 %	High
	handling in 3D	images	geometry		computation
	vision		optimization		cost
[24]	Handle occlusion	LiDAR	Memory-	88 %	Increased
	with temporal	sequences	augmented		latency
	context		detection		

[25]	Improve detection	KITTI,	Image + LiDAR +	88 %	Needs
. ,	in complex scenes	custom	roadside fusion		multiple
					sensors
[26]	Improve sparse-	4DRT	Multi-teacher	77.3 %	High training
	input detection		distillation		complexity
[27]	Improve robustness	KITTI,	Adversarial	73.8 %	Needs tuning;
	to lighting &	nuScenes	adaptive data		training
	occlusion		augmentation		overhead

The review of existing studies (Table 1) highlights that while numerous frameworks—ranging from AR-assisted perception to multi-sensor fusion and adversarial augmentation have improved detection accuracy, they remain constrained by computational cost, hardware dependence, and lack of dataset standardization. Most prior methods rely on proprietary or highly specialized setups, limiting reproducibility and industrial scalability. Furthermore, real-time or post-fabrication inspection pipelines are rarely optimized for lightweight deployment, which restricts their practical integration into additive manufacturing lines. These limitations collectively reveal a gap for an approach that balances high detection accuracy with computational efficiency and broad accessibility. Building on these insights, the present study proposes a deep learning—based defect detection framework using DenseNet201 to enhance post-printing quality control, minimize waste, and reduce reliance on manual inspection in industrial 3D printing environments.

3. Proposed Methodology

The research follows a structured methodology as shown in Figure 1: dataset acquisition and preparation, image preprocessing, data augmentation for better generalization, and data splitting for training and validation.

It evaluates three popular deep learning architectures using a two-stage training process, frozen base training followed by fine-tuning of top layers optimized for performance without overfitting. Classification is done using a SoftMax output layer to estimate the probability distribution of image defects.

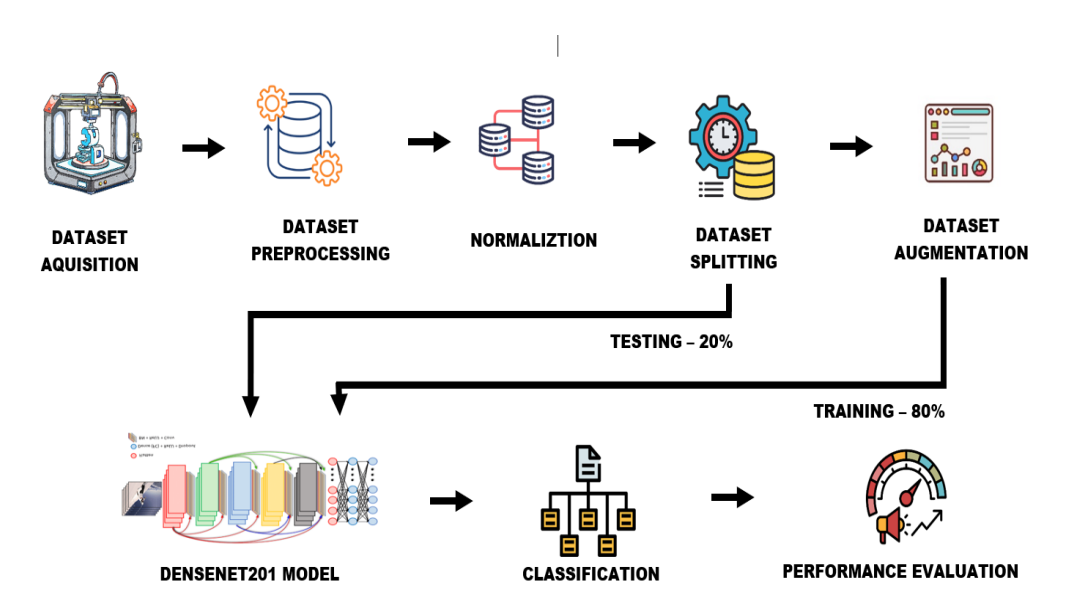


Figure 1. Proposed Methodology for 3D Object Detection Using Deep Learning

3.1. Dataset Acquisition

Fused Deposition Modeling (FDM) 3D Printing Defect Dataset [28] was created specifically for identifying and classifying frequent defects in FDM printed 3D objects, containing images of 3D prints displaying several defect types. The dataset has a total of 2,912 images, each labeled according to one of five defect types, providing foundational ground truth for supervised learning in defect detection and classification presented in Table 2. However, the dataset is moderately imbalanced before augmentation,

with certain classes, such as Off-Platform (91 samples), significantly underrepresented compared to Warping (538 samples) or Cracking (472 samples). This imbalance can bias model learning toward majority classes if not addressed. To mitigate this, targeted data augmentation was later applied to ensure uniform class representation and improve generalization performance during training.

Table 2. Dataset Details

Actual Name	Training Data Sample	Class Label
Cracking	472	Class
Layer Shifting	364	Class (2)
Off Platform	91	Class (3)
Stringing	447	Class (4)
Warping	538	Class (5)

3.2. Dataset Preprocessing

The preprocessing of data is an important process that makes raw data as good as possible before it is converted into a deep learning model. It includes the change of input data, transforming it and standardizing it, so that it is more likely to reach the model and learn valuable patterns. The following explains the progression of the preprocessing processes on the 3D printer dataset defect samples at the first stage. The images will be scaled to a standard size. Deep learning networks, particularly convolutional neural networks (CNNs), require that all input images be of the same dimension. In case the pictures in your data set are of different sizes, then the model will not be able to process them properly. The resizing, in turn, makes sure that all the images are of one size, which is essential to the effective processing.

3.3 Normalization

The subsequent preprocessing step is the normalization of the pixel intensities of images. The pixel values of most of the images in the dataset fall between 0 and 255 since most of them are usually stored in 8-bit format. Deep learning models are, however, more likely to perform better when the input features (here, the pixel values) are smaller and of constant scale. The large values of input can induce instability during training since the gradients of backpropagation might be very large or even very small, and this will result in slow convergence or an inability to converge.

Formula: For each pixel P, the normalized value P' is calculated as:

$$P'=P/255$$
 (1)

where P is the original pixel value and P' is the normalized value.

To fix this, we normalize our pixel values so we divide each pixel by 255. This normalizes the pixel values in the range [0, 255] to [0, 1].

3.4. Dataset Splitting

To assure that the model can be trained reliably and inferred reliably, the 3D printed object dataset was divided into three subsets: train, validate, and test. To evaluate the model's performance reliably, as well as help prevent overfitting, the train and validate subsets were created. The dataset was divided leveraging the validation split=0.2 parameter, where 80% of the data were allocated to the train set and 20% to the validation set. This separation ensures that a portion of the dataset remains unseen during training, allowing the model's generalization ability to new data to be measured accurately. During the data loading, the keras flow_from_directory function was set on the subset parameter to either "training" and "validation" during each corresponding load. Consequently, the two subsets could be separated automatically and consistently throughout the loads. During process of loading the models train and validating the model was monitored for each epoch. At each validation and monitoring interval of the model, modifications could be made to improve accuracy as well as correct for overfitting detected at the validation stage of training the model. The approach of long-term training along with a proper validation split enabled the model to realize a high validation accuracy of 00.93, demonstrating highly accurate defect detection under these varied and complex conditions.

3.5. Dataset Augmentation

Data augmentation plays a crucial role in improving model generalization and defect localization. To increase the diversity of limited training samples, targeted augmentation techniques were applied that specifically enhance the model's ability to detect small or spatially varied surface flaws. Random rotations (±40°) and horizontal flips improve orientation invariance, enabling recognition of defects from different

viewing angles. Width and height shifts (0.3 range) simulate off-centered prints, allowing the model to localize displaced or edge defects. Controlled zoom transformations (0.4 range) replicate scale variations, ensuring consistent detection of defects at multiple magnifications. These focused transformations effectively improved model robustness and reduced overfitting, allowing the DenseNet201 architecture to better identify fine-grained defect patterns across diverse printing conditions.

3.6. DenseNet201 Model

DenseNet201 is a densely connected convolutional neural network in which the output of each layer is directly linked to all subsequent layers, promoting feature reuse and mitigating vanishing-gradient issues. This compact connectivity improves learning efficiency and reduces redundant computations, making DenseNet architectures well-suited for detecting subtle surface variations in high-resolution 3D print images. Compared with lighter architectures such as MobileNetV2 or EfficientNetB0, DenseNet201 provides richer feature representations and higher resilience to gradient degradation, which are essential for capturing subtle geometric irregularities. Although MobileNet and EfficientNet are computationally faster, preliminary experiments in this study showed that they produced 5–8% lower validation accuracy and exhibited reduced sensitivity to micro-defects. DenseNet201 therefore offers a balanced compromise between accuracy and computational cost, achieving superior defect localization without requiring specialized high-end hardware. DenseNet alters this by having a dense connectivity pattern, such that each layer is given a concatenated output of all previous layers:

$$x_{l}=H_{L}([x_{0}, x_{1}, ..., x_{l-1}]$$
 (2)

where:

 x_l : Output of the l^{th} layer,

 H_L : Composite function (BatchNorm \rightarrow ReLU \rightarrow Conv),

 $x_0, x_1, ..., x_{l-1}$: Concatenation of feature maps from all previous layers.

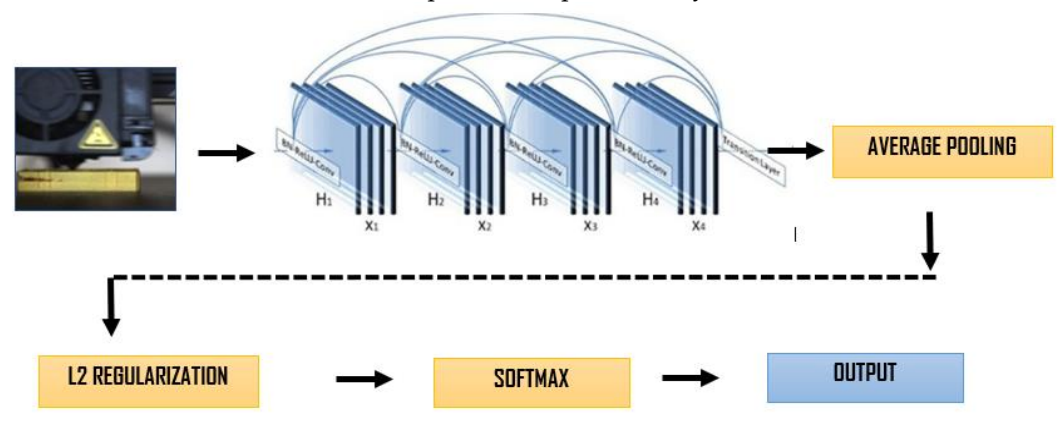


Figure 2. DenseNet201 Architecture

Each layer's computation includes:

$$H(x)=W_{l}*(Relu(BN(x)))$$
(3)

where:

 W_l : Learnable weight parameters for l^{th} layer,

BN: Batch normalization,

DenseNet201 is based on several layers, are shown in Figure 2.

Input to GlobalAveragePooling2D layer is a 3D tensor (A feature map), of size (H, W, C) where:

H is height of the feature map,

W is width of the feature map,

C is number of channels (or the depth of the feature map).

The layer computes the average value of each feature map across its spatial dimensions (height and width) for each channel.

Mathematically, the output is:

$$y_c = \frac{1}{H \times W} \sum_{i=1}^{H} \sum_{j=1}^{W} F_{i,j,c}$$
 (4)

where:

H and *W* are height and width of the feature map, y_c is index of the channel,

Feature MAP $_{i,c}$ is the pixel value at position (i, j) in channel c.

The resultant is a fixed-length vector containing one element per feature map (channel), regardless of the original size of the input image. As an example, an input with the dimensions (224, 224, 3) would output a (3,) dimensional vector, i.e., 1 average per channel.

3.7. Classification

After feature extraction by DenseNet201, several layers are appended to perform classification. The GlobalAveragePooling2D layer replaces traditional fully connected layers by averaging each feature map, significantly reducing parameters and preventing overfitting. It converts a 3D feature map into a fixed-length vector that summarizes spatial information, preserving essential features while enhancing model efficiency.

The BatchNormalization layer stabilizes learning by normalizing activations within mini-batches, ensuring consistent data distribution and accelerating convergence. It reduces internal covariate shift and serves as a light regularizer. Next, the Dropout layer introduces stochastic regularization by randomly deactivating 40% of neurons during training, preventing co-adaptation and improving generalization to unseen data.

The Dense (512, activation='ReLU') layer follows, learning complex, non-linear feature representations. The ReLU activation improves convergence speed and alleviates vanishing gradient issues.

$$ReL(x) = \max(0, x) \tag{5}$$

L2 regularization (weight decay) is applied to constrain weight magnitudes, minimizing overfitting and promoting smooth optimization. Into a normalized probability distribution, allowing clear interpretation of model confidence for each defect type. The class with the highest SoftMax score is chosen as the prediction.

$$Loss = Original\ Loss + \lambda \sum_{i} w^{2}$$
 (6)

This combination of pooling, normalization, dropout, and SoftMax layers ensures stable, efficient, and accurate classification of 3D printing defects, enhancing model reliability and interpretability in real-world applications.

$$Softmax (x)_i = \frac{e^x}{\sum_{i=1}^k e^{x_i}}$$
 (7)

Where x_1 is the output of the ith neuron of the last layer, and the denominator is the sum of the ith outputs of all classes. It is arranged such that the output of each element is between 0 and 1, and the outputs add up to 1 (therefore, they can be interpreted as probabilities of classes).

4. Result and Discussion

This section presents the results obtained from implementing the DenseNet201 deep learning model for defect detection in Fused Deposition Modeling (FDM) 3D printed objects using the Kaggle FDM 3D Printing Defect Dataset. The primary objective was to enhance the accuracy and reliability of defect identification through deep learning-based automation. The dataset contained labeled images of 3D printed parts representing different types of surface and structural defects. The model was trained and validated on these images after applying preprocessing steps such as resizing, normalization, and data augmentation to improve generalization. Performance was evaluated using standard metrics, including accuracy, precision, recall, and F1-score, as shown in Figure 3.

Precision =
$$\frac{(\text{True Positive})}{(\text{True Positive} + \text{False Positive})}$$

$$\text{Recall} = \frac{(\text{True Positive} + \text{False Negative})}{(\text{True Positive} + \text{False Negative})}$$

$$\text{F - 1 Score} = \frac{2*(\text{Precision * Recall})}{(\text{Precision+Recall})}$$

$$\text{Accuracy} = \frac{(\text{True Positive+True Negative})}{(\text{Total Positive+Total Negative})}$$

$$\text{(11)}$$

$$\text{results highlight the effectiveness of the proposed model in capturing fine-graine}$$

These results highlight the effectiveness of the proposed model in capturing fine-grained defect characteristics that are often overlooked by manual inspection. In addition to accuracy-based performance, the computational efficiency of the proposed model was also evaluated to assess its suitability for industrial environments. Beyond accuracy, the computational performance of the DenseNet201 framework was

evaluated to confirm its suitability for industrial implementation. All experiments were conducted on a 12th gen Intel CoreTM i5-12400 (2.50 GHz) processor, with 16 GB RAM & 512 GB SSD storage to ensure high data throughput. While training can be performed on a CPU, using a dedicated GPU such as NVIDIA GTX 1660 significantly reduces training time and improves model responsiveness. Under these conditions, the fine-tuned DenseNet201 achieved an average inference time of 38 ms per image on an NVIDIA RTX 3060 GPU, allowing near real-time inspection of printed parts. With approximately 20 million trainable parameters, the model maintains a balanced trade-off between complexity and detection precision. The total training duration was 3 to 4 hours for 50 epochs, demonstrating that the network can be retrained efficiently when new defect types are introduced. These results confirm that the proposed approach is not only accurate but also computationally feasible for post-fabrication defect detection in modern manufacturing workflows.

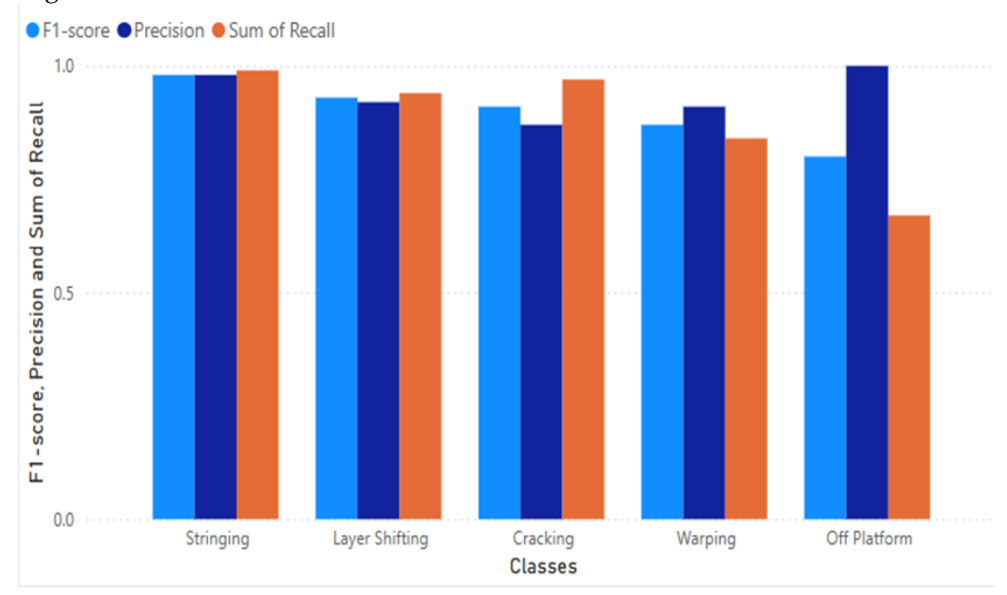


Figure 3. Precision, Recall, and F1-Score

Class-wise results are presented in Table 3, given below.

Table 3. Precision, Recall, and F1-Score

	Precision	Recall	F-1 score	Support
Class	0.87	0.97	0.91	94
Class (2)	0.92	0.94	0.93	72
Class (3)	1	0.67	0.80	18
Class (4)	0.98	0.99	0.98	89
Class (5)	0.91	0.84	0.87	107
accuracy			0.92	380
macro avg	0.93	0.88	0.90	380
weighted avg	0.91	0.92	0.92	380

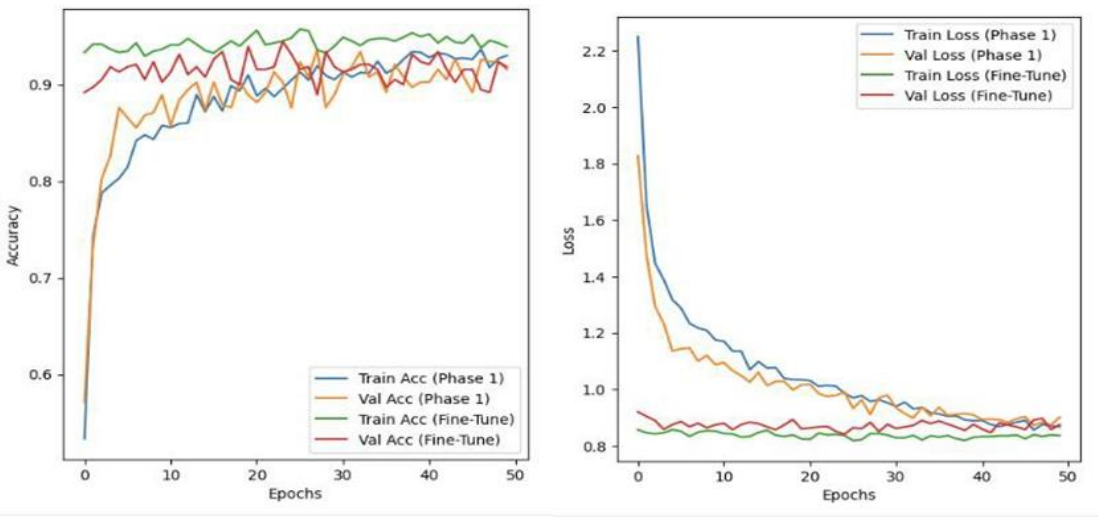


Figure 4. Training & Validation Curves of 3d Object Detection

A confusion matrix is a way the true positives, false positives, true negatives, and false negatives of each model are visually represented. It helps to evaluate where the model is making errors, especially in distinguishing between defective and non-defective prints, as shown in Figure 5.

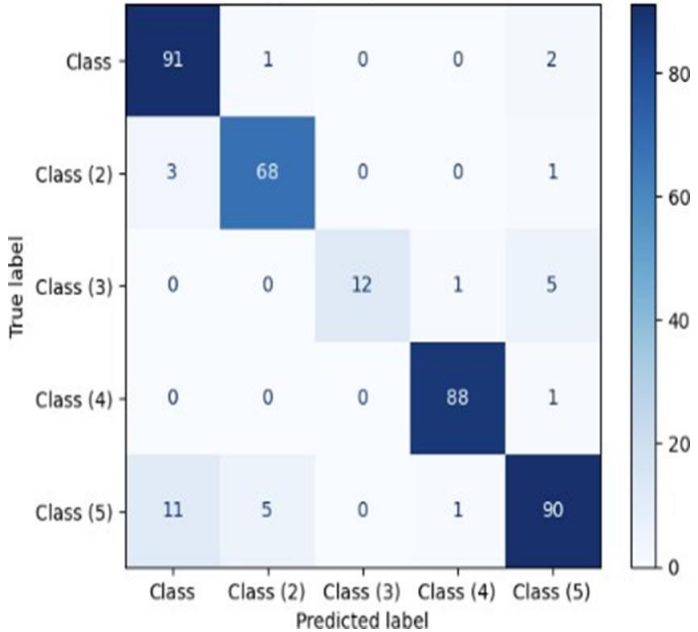


Figure 5. Confusion Matrix of 3D object detection

4.1. Comparison with existing techniques

DenseNet architectures offer several advantages that make them particularly effective for tasks such as defect detection in 3D printing. One key benefit is feature reuse, which allows each layer to access the outputs of all preceding layers. This design avoids redundant computation by reusing learned features, leading to improved computational efficiency and richer feature representations as presented in Table 4.

Table 4. Comparison of the proposed technique with the existing techniques

Paper	Year	Model	Results
[29]	2018	VoxelNet	77.5%
[30]	2020	PV-RCNN	84.4%
[31]	2020	3DSSD	85.7%
[32]	2017	PointNet	89.2%
[33]	2017	PointNet++	91.9%
Proposed Work	2025	DenseNet201	93%

Compared to existing studies, the proposed research leverages a more standardized and publicly available dataset FDM 3D Printer Defect Dataset from Kaggle while many other works rely on custom datasets with limited accessibility. This ensures reproducibility and benchmarking opportunities for future researchers. Additionally, while several studies [34-39] used traditional CNNs or lighter architectures like MobileNetV2 [34] and YOLOv4-Tiny [35], this study applies DenseNet201, a deeper pretrained model, combined with fine-tuning, advanced data augmentation, label smoothing, and learning rate scheduling to enhance performance. While some papers focused on defect detection, they often sacrificed classification accuracy or did not reach a consistent 93% accuracy across multiple classes, as achieved in this work. The current model is limited to detecting defects after the printing process. It does not support real-time monitoring, which is essential for early fault detection and prevention during printing. Lightweight models like YOLOv4-Tiny or MobileNetV3 can be explored for integration into live monitoring systems. The dataset used has an imbalanced class distribution, especially for underrepresented classes like "Off Platform", which may negatively affect the model's generalization on unseen or rare defect types. While classification accuracy is high, the model lacks explainable AI (XAI) components that help users understand why a certain defect was detected. Integrating LIME or Grad-CAM could enhance transparency.

5. Conclusion

This study aims to propose a deep learning-based method to achieve this in the quest of gaining a much better-quality control process in 3D printing to enhance the efficiency of manufacturing, waste reduction, and lower costs of applying traditional defect identification techniques. Automation of the defect identification is another way through which manufacturers can deliver higher quality and a more consistent production of 3D printed objects by eliminating the intensity of the challenge of existing traditional inspection methods. This research explored the application of deep learning techniques, particularly convolutional neural networks (CNNs), to enhance 3D printing through automated defect detection. The study proved the usefulness of transfer learning and fine-tuning on pre-trained networks such as DenseNet201 to identify defects in 3D printed products. The findings revealed that deep learningbased models have the potential to enhance the accuracy and reliability of defect detection to a significant degree, and this aspect makes the process more efficient and cost-effective. Data augmentation and optimization methods have allowed the model to generalize well and minimize overfitting, which makes it a solid solution to practical industrial scenarios. Detecting defects with the assistance of AI not only improves the quality control in 3D printing but also allows accelerating the production process and decreasing the amount of material waste, solving some of the fundamental issues that trouble the industry. Its performance was measured with the help of standard metrics, such as accuracy, precision, recall, F1score, and confusion matrix, which allowed gaining a detailed picture of its functionality. Future work can be on the integration of AI models into the 3D printing process to detect defects in real-time, decreasing the necessity of post-processing inspection and guaranteeing quality standards during production. Investigating the possibility of combining optical and thermal imaging may improve the quality of defect detection, as it may allow better coverage of the printed objects and ultimately increase the accuracy of detecting various defects.

References

- 1. Carrasco-Correa, E.J., Vergara-Barberán, M., Miró, M., and Herrero-Martínez, J.M.: 'Introduction to 3D printing from the analytical chemistry viewpoint': '3D Printing in Analytical Chemistry' (Elsevier, 2025), pp. 3-15
- 2. Ben Rezg, M., Nasser, M., Othmani, R., and Montagne, A.: 'Multi-criteria selectivity of PLA polymer 3D printing parameters: impact on the roughness of finished surfaces', Progress in Additive Manufacturing, 2025, pp. 1-23
- 3. Błaszczykowski, M., Majerek, D., Sędzielewska, E., Tomiło, P., and Pytka, J.: 'A novel machine learning system for early defect detection in 3D printing', Advances in Science and Technology. Research Journal, 2025, 19, (3)
- 4. Usamentiaga, R., Lema, D.G., Pedrayes, O.D., and Garcia, D.F.: 'Automated surface defect detection in metals: a comparative review of object detection and semantic segmentation using deep learning', IEEE Transactions on Industry Applications, 2022, 58, (3), pp. 4203-4213
- 5. Jadayel, M., and Khameneifar, F.: 'Increasing 3D Printing Accuracy Through Convolutional Neural Network-Based Compensation for Geometric Deviations', Machines, 2025, 13, (5), pp. 382
- 6. Tang, M., Ting, K.C., and Rashidi, N.H.: 'DenseNet201-based waste material classification using transfer learning approach', Applied Mathematics and Computational Intelligence (AMCI), 2024, 13, (2), pp. 113-120
- 7. Ahmed, L., Iqbal, M.M., Aldabbas, H., Khalid, S., Saleem, Y., and Saeed, S.: 'Image data practices for semantic segmentation of breast cancer using deep neural network', Journal of Ambient Intelligence and Humanized Computing, 2023, 14, (11), pp. 15227-15243
- 8. Pičuljan, N., and Car, Ž.: 'Machine learning-based label quality assurance for object detection projects in requirements engineering', Applied Sciences, 2023, 13, (10), pp. 6234
- 9. Sezer, A., and Altan, A.: 'Detection of solder paste defects with an optimization-based deep learning model using image processing techniques', Soldering & Surface Mount Technology, 2021, 33, (5), pp. 291-298
- 10. Nebiker, S., Meyer, J., Blaser, S., Ammann, M., and Rhyner, S.: 'Outdoor mobile mapping and AI-based 3D object detection with low-cost RGB-D cameras: The use case of on-street parking statistics', Remote Sensing, 2021, 13, (16), pp. 3099
- 11. Muzahid, A., Han, H., Zhang, Y., Li, D., Zhang, Y., Jamshid, J., and Sohel, F.: 'Deep learning for 3D object recognition: A survey', Neurocomputing, 2024, 608, pp. 128436
- 12. Alzubaidi, L., Zhang, J., Humaidi, A.J., Al-Dujaili, A., Duan, Y., Al-Shamma, O., Santamaría, J., Fadhel, M.A., Al-Amidie, M., and Farhan, L.: 'Review of deep learning: concepts, CNN architectures, challenges, applications, future directions', Journal of big Data, 2021, 8, (1), pp. 53
- 13. Sorensen, L., Nielsen, M., Lo, P., Ashraf, H., Pedersen, J.H., and De Bruijne, M.: 'Texture-based analysis of COPD: a data-driven approach', IEEE transactions on medical imaging, 2011, 31, (1), pp. 70-78
- 14. Chen, Y., Ding, Y., Zhao, F., Zhang, E., Wu, Z., and Shao, L.: 'Surface defect detection methods for industrial products: A review', Applied Sciences, 2021, 11, (16), pp. 7657
- 15. Wang, Y., Huang, J., Wang, Y., Feng, S., Peng, T., Yang, H., and Zou, J.: 'A CNN-based adaptive surface monitoring system for fused deposition modeling', IEEE/ASME Transactions On Mechatronics, 2020, 25, (5), pp. 2287-2296
- 16. Kandel, I., and Castelli, M.: 'How deeply to fine-tune a convolutional neural network: a case study using a histopathology dataset', Applied Sciences, 2020, 10, (10), pp. 3359
- 17. Salim, F., Saeed, F., Basurra, S., Qasem, S.N., and Al-Hadhrami, T.: 'DenseNet-201 and Xception pre-trained deep learning models for fruit recognition', Electronics, 2023, 12, (14), pp. 3132
- 18. Shahrubudin, N., Lee, T.C., and Ramlan, R.: 'An overview on 3D printing technology: Technological, materials, and applications', Procedia manufacturing, 2019, 35, pp. 1286-1296
- 19. Kristiawan, R.B., Imaduddin, F., Ariawan, D., Ubaidillah, and Arifin, Z.: 'A review on the fused deposition modeling (FDM) 3D printing: Filament processing, materials, and printing parameters', Open Engineering, 2021, 11, (1), pp. 639-649
- 20. Deshmane, S., Kendre, P., Mahajan, H., and Jain, S.: 'Stereolithography 3D printing technology in pharmaceuticals: a review', Drug Development and Industrial Pharmacy, 2021, 47, (9), pp. 1362-1372
- 21. Lekurwale, S., Karanwad, T., and Banerjee, S.: 'Selective laser sintering (SLS) of 3D printlets using a 3D printer comprised of IR/red-diode laser', Annals of 3D Printed Medicine, 2022, 6, pp. 100054
- 22. Li, V., Siniosoglou, I., Karamitsou, T., Lytos, A., Moscholios, I.D., Goudos, S.K., Banerjee, J.S., Sarigiannidis, P., and Argyriou, V.: 'Enhancing 3D object detection in autonomous vehicles based on synthetic virtual environment analysis', Image and Vision Computing, 2025, 154, pp. 105385

- 23. Li, Z., Yu, H., Ding, Y., Qiao, J., Azam, B., and Akhtar, N.: 'GO-N3RDet: Geometry Optimized NeRF-enhanced 3D Object Detector', in Editor (Ed.)^(Eds.): 'Book GO-N3RDet: Geometry Optimized NeRF-enhanced 3D Object Detector' (2025, edn.), pp. 27211-27221
- 24. Agro, B., Casas, S., Wang, P., Gilles, T., and Urtasun, R.: 'MAD: Memory-Augmented Detection of 3D Objects', in Editor (Ed.)^(Eds.): 'Book MAD: Memory-Augmented Detection of 3D Objects' (2025, edn.), pp. 1449-1460
- 25. Xia, B., Zhou, J., Kong, F., You, Y., Yang, J., and Lin, L.: 'Enhancing 3D object detection through multi-modal fusion for cooperative perception', Alexandria Engineering Journal, 2024, 104, pp. 46-55
- 26. Song, S.-H., Paek, D.-H., Dao, M.-Q., Malis, E., and Kong, S.-H.: 'Enhanced 3D Object Detection via Diverse Feature Representations of 4D Radar Tensor', arXiv preprint arXiv:2502.06114, 2025
- 27. Li, S., Li, J., Fu, J., and Chen, Q.: 'Boosting 3D Object Detection with Adversarial Adaptive Data Augmentation Strategy', Sensors, 2025, 25, (11), pp. 3493
- 28. Khan, M.F., Alam, A., Siddiqui, M.A., Alam, M.S., Rafat, Y., Salik, N., and Al-Saidan, I.: 'Real-time defect detection in 3D printing using machine learning', Materials Today: Proceedings, 2021, 42, pp. 521-528
- 29. Zhou, Y., and Tuzel, O.: 'Voxelnet: End-to-end learning for point cloud based 3d object detection', in Editor (Ed.)^(Eds.): 'Book Voxelnet: End-to-end learning for point cloud based 3d object detection' (2018, edn.), pp. 4490-4499
- 30. Shi, S., Guo, C., Jiang, L., Wang, Z., Shi, J., Wang, X., and Li, H.: 'Pv-rcnn: Point-voxel feature set abstraction for 3d object detection', in Editor (Ed.)^(Eds.): 'Book Pv-rcnn: Point-voxel feature set abstraction for 3d object detection' (2020, edn.), pp. 10529-10538
- 31. Yang, Z., Sun, Y., Liu, S., and Jia, J.: '3dssd: Point-based 3d single stage object detector', in Editor (Ed.)^(Eds.): 'Book 3dssd: Point-based 3d single stage object detector' (2020, edn.), pp. 11040-11048
- 32. Qi, C.R., Su, H., Mo, K., and Guibas, L.J.: 'Pointnet: Deep learning on point sets for 3d classification and segmentation', in Editor (Ed.)^(Eds.): 'Book Pointnet: Deep learning on point sets for 3d classification and segmentation' (2017, edn.), pp. 652-660
- 33. Qi, C.R., Yi, L., Su, H., and Guibas, L.J.: 'Pointnet++: Deep hierarchical feature learning on point sets in a metric space', Advances in neural information processing systems, 2017, 30
- 34. Dong, K., Zhou, C., Ruan, Y., and Li, Y.: 'MobileNetV2 model for image classification', in Editor (Ed.)^(Eds.): 'Book MobileNetV2 model for image classification' (IEEE, 2020, edn.), pp. 476-480
- 35. Jiang, Z., Zhao, L., Li, S., and Jia, Y.: 'Real-time object detection method based on improved YOLOv4-tiny', arXiv preprint arXiv:2011.04244, 2020
- 36. Z. Awais *et al.*, "ISCC: Intelligent Semantic Caching and Control for NDN-Enabled Industrial IoT Networks," in *IEEE Access*, vol. 13, pp. 169881-169898, 2025, doi: 10.1109/ACCESS.2025.3614984.
- 37. Zubair, M.; Hussain, M.; Albashrawi, M.A.; Bendechache, M.; Owais, M. A comprehensive review of techniques, algorithms, advancements, challenges, and clinical applications of multi-modal medical image fusion for improved diagnosis. Computer Methods and Programs in Biomedicine. 2025, 272, 109014. https://doi.org/10.1016/j.cmpb. 2025.109014
- 38. Hussain, M., Chen, C., Hussain, M. et al. Optimised knowledge distillation for efficient social media emotion recognition using DistilBERT and ALBERT. Sci Rep 15, 30104 (2025). https://doi.org/10.1038/s41598-025-16001-9
- 39. Zubair, M., Owais, M., Hassan, T. *et al.* An interpretable framework for gastric cancer classification using multichannel attention mechanisms and transfer learning approach on histopathology images. *Sci Rep* **15**, 13087 (2025). https://doi.org/10.1038/s41598-025-97256-0.